PLASMA-WAVE INSTABILITY IN NARROW-GAP SEMICONDUCTORS

P. A. Wolff
Bell Telephone Laboratories, Incorporated, Holmdel, New Jersey
(Received 8 October 1969)

In narrow-gap semiconductors, the energy of conduction-electron plasma oscillations can be made equal to the band gap by doping. When such a crystal is pumped with an electron beam or light wave, stimulated emission of plasma waves takes place. Estimates of growth rate suggest that, in $Pb_{1-x}Sn_xSe$ and $Pb_{1-x}Sn_xTe$ alloys, collisional losses can be overcome and the plasma waves excited to high amplitude.

In the past few years, small-band-gap semiconductors and semimetals have been studied with increasing vigor. The properties of materials such as InSb, PbTe, Bi, $Pb_{1-x}Sn_xTe$, $Pb_{1-x}Sn_xSe$, $Hg_{1-x}Cd_xTe$, and the Bi-Sb alloys have been investigated in detail,[1] and several devices whose operation depends upon the small-band-gap property have been demonstrated.[2] A particularly interesting subclass of these materials is that of the alloys, such as $Pb_{1-x}Sn_xSe$ and $Pb_{1-x}Sn_xTe$, in which a direct energy gap can be continuously varied, through zero, in a crystal with simple band structure.[1d,2] This feature makes it possible, with appropriate choice of composition, to adjust the band gap (E_G) to coincide with other important frequencies in the crystal. This paper will discuss some of the implications of choosing E_G equal to the plasma frequency (ω_p) of the conduction electrons in such a material.[3] In particular, we will consider the behavior of plasma waves when the crystal is pumped by light or an electron beam to excite electrons from the valence to the conduction bands. It will be shown that, under these circumstances, the plasma waves can become unstable and rapidly grow in amplitude. Pumping inverts the band-edge transition. Stimulated emission of plasma waves then occurs, if $E_G \simeq \omega_p$, because the Coulomb field of the wave has a matrix element which induces interband transitions. This process is a strong one, even at modest pumping levels. It appears possible, in both the $Pb_{1-x}Sn_xSe$ and $Pb_{1-x}Sn_xTe$ systems, to overcome the collisional damping of the plasma waves and excite them to high amplitude.

To discuss the instability, we consider a simple band structure such as that of $Pb_{1-x}Sn_xSe$. A band-edge point of the $Pb_{1-x}Sn_xSe$ system is illustrated in Fig. 1(a). The minima of the conduction band are directly above the maxima of the valence band at the L points of the Brillouin zone.[2] For concreteness, we consider a crystal with n-type doping, and assume the plasma frequency of the conduction electrons about equal to the energy gap. In a cubic crystal the plasma frequency is independent of propagation direction and is given by the formula

$$\omega_p^2 = \frac{4\pi e^2}{\epsilon_0}\sum_i (n_{0i}\vec{\vec{\alpha}}_i) \equiv \frac{4\pi n_0 e^2}{\epsilon_0 m^*}, \tag{1}$$

where n_{0i} is the electron density in the ith conduction-band minimum, and $\vec{\vec{\alpha}}_i = \partial^2 E_i/\partial\vec{k}\partial\vec{k}$ is the reciprocal effective-mass tensor for that minimum. $n_0 = \sum_i (n_{0i})$, and $1/m^* = \frac{1}{4}\sum_i (\vec{\vec{\alpha}}_i)$. In all these formulas, the masses and effective-mass tensors are evaluated at the Fermi surface. Band nonparabolicity can cause these values to differ by sizable factors from the corresponding quantities at the band-edge points.

Let us now imagine that, with an electron beam or light wave, we excite electrons from the valence to the conduction bands. The excited particles thermalize, via electron-electron interactions, in about 3×10^{-13} sec. If this time is appreciably shorter than the recombination time the distribution shown in Fig. 1(b) results. Usually, this condition is easily satisfied. When $E_G \simeq \omega_p$, the recombination time is shortened by spontaneous emission of plasmons. For the example discussed later it becomes about 2×10^{-12} sec, which is still considerably longer than the

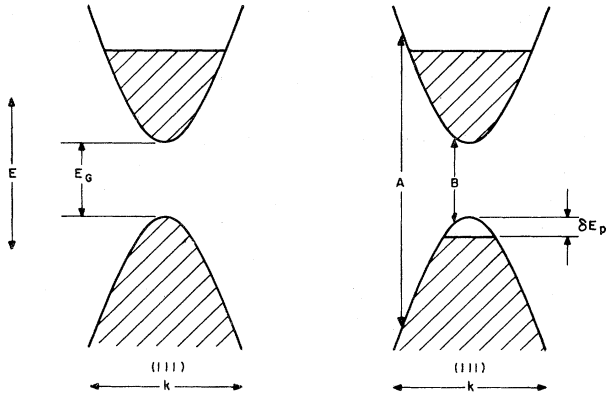

FIG. 1. Band structure of $Pb_{1-x}Sn_xSe$ alloys (a) before and (b) after beam pumping.

thermalization time. Thus, we will use the velocity distribution of Fig. 1(b) in our calculations. It should be emphasized that the hole densities we are envisaging here are relatively small—perhaps 1% of the electron density. Typical values are $n_0 = 10^{17}$-$10^{18}/\mathrm{cm}^3$; p(hole density) $= 10^{15}$-$10^{16}/\mathrm{cm}^3$.

To investigate the behavior of plasma waves in this medium, we consider the longitudinal, wave-vector-dependent, dielectric function of the electron gas. In the random-phase approximation, this function is given by the expression[4]

$$\epsilon(\vec{k},\omega) = 1 - \left(\frac{4\pi e^2}{k^2}\right) \sum_{\substack{\vec{p} \\ \lambda,\mu}} \frac{[f_\lambda(\vec{p}-\vec{k}) - f_\mu(\vec{p})]\, |\langle \vec{p}, \mu | e^{i\vec{k}\cdot\vec{r}} | \vec{p}-\vec{k}, \lambda\rangle|^2}{[\omega + E_\lambda(\vec{p}-\vec{k}) - E_\mu(\vec{p})]}, \tag{2}$$

where $E_\mu(\vec{p})$ is the energy of an electron with crystal momentum $\vec{p}$ in the band μ, and $f_\mu(\vec{p})$ is the occupation number of this state. The frequencies of the collective modes are determined by the condition $\epsilon(\vec{k},\omega) = 0$.

For the plasma illustrated in Fig. 1(b), three types of matrix elements contribute to $\epsilon(\vec{k},\omega)$: interband terms involving deep-lying valence electrons [transitions such as those indicated by arrow A in Fig. 1(b)], intraband terms which give rise to the plasma contribution to $\epsilon(\vec{k},\omega)$, and, finally, interband terms in which electrons near the band-edge point in the conduction band fall into the small hole pocket at the top of the valence band [arrow B of Fig. 1(b)]. These terms yield the expression (at zero temperature)

$$\epsilon(\vec{k},\omega) = \epsilon_0 - \frac{\epsilon_0 \omega_p^2}{\omega^2} - \left(\frac{4\pi e^2}{k^2}\right) \int \frac{2d^3p}{(2\pi)^3} |\langle \vec{p}, v | e^{i\vec{k}\cdot\vec{r}} | \vec{p}-\vec{k}, c\rangle|^2 \times \left[\frac{1}{E_v(\vec{p}) + E_c(\vec{p}-\vec{k}) + E_G + \omega} + \frac{1}{E_v(\vec{p}) + E_c(\vec{p}-\vec{k}) + E_G - \omega}\right], \tag{3}$$

where the d^3p integration extends over the hole pockets in the valence band. $E_c(\vec{p})$ and $E_v(\vec{p})$ are the energies of conduction- and valence-band states. For simplicity, we have ignored the (usually small) frequency dependence of ϵ_0. It has also been assumed that k is small compared with the Fermi-Thomas wave vector of the electron gas; so there is no dispersion or Landau damping of the plasma wave. The interband matrix elements can easily be evaluated with $\vec{k}\cdot\vec{p}$ perturbation theory. One finds

$$|\langle \vec{p}, v | e^{i\vec{k}\cdot\vec{r}} | \vec{p}-\vec{k}, c\rangle|^2 \simeq (\vec{k}\cdot\vec{\pi}_{cv})^2/(mE_G)^2, \tag{4}$$

where $\vec{\pi}_{cv}$ is the interband matrix element of the momentum operator at the band-edge point. Within the two-band model, the combination $\vec{\pi}_{cv}\vec{\pi}_{vc}/m^2E_G$ is essentially the effective-mass tensor, $\partial^2 E/\partial\vec{k}\partial\vec{k}$, at the band edge. When Eq. (4) is substituted into Eq. (3) the last term remains finite in the limit $k = 0$. The interband matrix element of the operator $e^{i\vec{k}\cdot\vec{r}}$ goes linearly to zero as $k \to 0$, but this effect is balanced by the fact that the potential of a plasma wave varies as k^{-1} in the small-k limit.

With these points in mind, Eq. (3) can be rewritten in the form

$$\epsilon(\vec{k},\omega) \simeq \epsilon_0 - \frac{\epsilon_0\omega_p^2}{\omega^2} - 4\pi e^2 \int \rho(E) \left[\frac{1}{E + E_G + \omega} + \frac{1}{E + E_G - \omega}\right] dE, \tag{5}$$

where

$$\rho(E) = \sum_i \int \frac{d^3p_i}{4\pi^3} \frac{(\vec{k}\cdot\vec{\pi}_{cvi})^2}{(mE_Gk)^2}\, \delta(E - E_{vi}(\vec{p}) - E_{ci}(\vec{p}-\vec{k})) \tag{6}$$

is a weighted, joint density of states for conduction- to valence-band transitions. The subscript i refers to the ith valence-band maximum. Equation (5) implies that, if ω is a solution of the equation $\epsilon(\vec{k},\omega) = 0$, ω^* is also a root. Thus, the condition for instability in this collisionless model is that ω be complex.

The transcendental equation, $\epsilon(\vec{k},\omega) = 0$, is a complicated one, even when $k = 0$. However, it can be approximately solved in the limiting cases where the imaginary part of $\omega(=\omega_1 + i\omega_2)$ is either large or small compared with the range of the E integration in Eq. (5). This range is twice the Fermi energy of the hole pockets [$2\delta E_p$ of Fig. 1(b)] if $k = 0$, and increases with k. If $\omega_2 \gg \delta E_p$, Eq. (5) is evaluated

by omitting the E dependence of the denominators. The resulting expression for $\epsilon(\vec{k}, \omega)$ is

$$\epsilon(\vec{k}, \omega) \simeq \epsilon_0 \left\{ 1 - \frac{\omega_p^2}{\omega^2} - \omega_p^2 \left(\frac{p}{n_0} \right) \left(\frac{m_{FS}^*}{m_{BE}^*} \right) \left(\frac{1}{E_G^2 - \omega^2} \right) \right\}, \quad (7)$$

where m_{FS}^* is the effective mass at the Fermi surface [Eq. (1)] and m_{BE}^* the mass at the band-edge point. When $\omega_p = E_G$, the roots of Eq. (7) are

$$\omega \simeq \omega_p \left\{ 1 \pm \frac{i}{2} \left[\left(\frac{p}{n_0} \right) \left(\frac{m_{FS}^*}{m_{BE}^*} \right) \right]^{1/2} \right\}. \quad (8)$$

On the other hand, when $\omega_2 \ll \delta E_p$, the imaginary part of Eq. (5) is

$$\mathrm{Im}\epsilon(\vec{k}, \omega) \simeq \frac{2\epsilon_0 \omega_p^2 \omega_2}{\omega_1^3} - \frac{\pi \omega_2}{|\omega_2|} 4\pi e^2 \rho(\omega_1 - E_G). \quad (9)$$

The real part of Eq. (5) indicates that, at low pumping levels ($p/n_0 \ll 1$), $\omega_1 \simeq \omega_p$. Thus

$$\omega_2 \simeq \pm \tfrac{1}{2} \pi (4\pi e^2/\epsilon_0) \omega_p \rho(\omega_p - E_G). \quad (10)$$

Equations (8) and (10) give the limiting behavior of the growth rate. In intermediate cases we will assume that ω_2 is equal to the smaller of the values predicted by these formulas. Detailed calculations indicate that this approximation is often quite good, and that in the worst cases it overestimates ω_2 by about 30%.

As an example, we consider the alloy $Pb_{0.81}Sn_{0.19}Se$ discussed in Ref. 2. With $n_0 = 10^{18}/\mathrm{cm}^3$, $\omega_p \cong E_G \cong 0.03$ eV. Using the two-band model,[5] one estimates that $m_{FS}^*/m_{BE}^* = 4$. If $p = 10^{16}/\mathrm{cm}^3$, Eq. (8) yields the value $|\omega_2| \simeq 5 \times 10^{12}$ sec^{-1}. A similar figure is obtained from Eq. (10) if $\omega_p - E_G$ is equal to $\delta E_p/2$. Thus $|\omega_2| \simeq 5 \times 10^{12}$ sec^{-1} is a reasonable value for the growth rate. For instability actually to occur, this rate must exceed collisional losses which, for plasma waves, are determined by $1/2\tau$, where τ is the electron collision time. The net growth rate is then $\omega_2 - 1/2\tau$. In our example, instability occurs if $\tau > 10^{-13}$ sec. Measurements of optical absorption[6] in PbTe crystals with 10^{17} electrons/cm^3 give free-carrier absorption coefficients in the range 2-10 cm^{-1}. The corresponding high-frequency collision times are $\tau = 10^{-12} - (2 \times 10^{-13})$ sec. To the author's knowledge, no such experiments have been performed in $Pb_{1-x}Sn_xSe$ or $Pb_{1-x}Sn_xTe$ alloys, but if the PbTe results can be extrapolated to these systems, the instability will be excited at pumping levels below $p = 10^{16}/\mathrm{cm}^3$.

As we have indicated, the population inversion which drives the instability is produced by pumping the crystal with an electron beam or light wave. The pump generates hot electrons and holes, which subsequently thermalize to the distribution of Fig. 1(b). During the thermalization process, plasma waves are excited in the electron gas. This excitation, however, should be clearly distinguished from the instability itself. The former is an incoherent process, in which energy is deposited in all possible collective modes of the system, and no particular plasma wave is excited to high amplitude. On the other hand, the instability is coherent and drives a small fraction of the collective modes. Under most conditions, these will be modes of low k, since the function $\rho(E)$ decreases as k increases. Preliminary calculations suggest that the unstable modes can be confined to the range $k \leq 10^5$ cm^{-1}. It is even possible that, in a finite geometry, one could use depolarizing fields to split a few, very low k modes from the continuum and selectively excite these. Among such modes are electric dipole oscillations of the whole plasma in the crystal. These modes radiate strongly. Thus, it is conceivable that the instability could be used as a source of infrared radiation.

The author wishes to thank H. O. Pollak for a number of stimulating discussions of the equation $\epsilon(\vec{k}, \omega) = 0$.

[1]There is much literature concerning such materials. We cite only a few of the most relevant articles. Further bibliography will be found in these references.

[1a]InSb, InAs, etc.: Properties of the III-V compounds are described in the series of books Semiconductors and Semimetals, edited by R. K. Willardson and A. C. Beer (Academic, New York, 1966-1967), Vols. I-III.

[1b]PbTe: L. Kleinman and P. J. Lin, in Proceedings of the Seventh International Conference on the Physics of Semiconductors, Paris, France, 1964 (Dunod, Paris, 1964), pp. 63-68; G. W. Pratt and L. G. Ferreira, ibid., pp. 69-76; J. O. Dimmock and G. B. Wright, ibid., pp. 77-81; K. F. Cuff, M. R. Ellett, and C. D. Kuglin, ibid., pp. 677-684.

[1c]Bi: B. Lax and J. B. Mavroides, in Advances in Solid State Physics, edited by F. Seitz and D. Turnbull (Academic, New York, 1960), Vol. 11.

[1d](Pb, Sn)Se, (Pb, Sn)Te: J. O. Dimmock, I. Melngailis, and A. J. Strauss, Phys. Rev. Letters. 16, 1193

(1966).

[1e](Hg, Cd)Te; M. Rodot, in Proceedings of the Ninth International Conference on the Physics of Semiconductors, Leningrad, U. S. S. R., 1967 ("Nauka," Leningrad, U. S.S.R., 1968) p. 639.

[1f]Bi-Sb alloys: S. Golin, Phys. Rev. 176, 830 (1968); A. L. Jain, Phys. Rev. 144, 1518 (1959).

[2]See Dimmock, Melngailis, and Strauss, Ref. 1d; also A. R. Calawa, J. O. Dimmock, T. C. Harmon, and I. Melngailis, Phys. Rev. Letters 23, 7 (1969); C. Verie, R. Granger, Compt. Rend. 216, 3349 (1965); I. Melngailis and A. J. Strauss, Appl. Phys. Letters 8, 179 (1966); C. Verie and J. Ayas, Appl. Phys. Letters 10, 241 (1967).

[3]We use units such that $\hbar = 1$.

[4]D. Pines, Elementary Excitations in Solids (Benjamin, New York, 1964).

[5]B. Lax and J. G. Mavroides, in Advances in Solid State Physics, edited by F. Seitz and D. Turnbull (Academic, New York, 1960).

[6]C. K. N. Patel and R. E. Slusher, Phys. Rev. 177, 1200 (1969).

HALL EFFECT AND RESISTIVITY ANISOTROPY IN Ni ALLOYS

I. A. Campbell
Physique des Solides,* Faculté des Sciences, 91 Orsay, France
(Received 23 October 1969)

Experimental data on the Hall effect and the resistivity anomaly are analyzed using the two-current conduction model; information is obtained on the Fermi surfaces of Ni.

Recent dilute-alloy resistivity experiments[1-3] have demonstrated the correctness of Mott's parallel-current model[4] for conduction in ferromagnetic metals, particularly Ni; thermoelectric-power[5] and thermal-conductivity[6] measurements give results consistent with the resistivity data. This Letter outlines an interpretation of galvanomagnetic data in Ni alloys, using the same model together with information on impurity scattering derived from the resistivity experiments.

For present purposes, the model[1,7] can be summarized as follows: At low temperatures spin-up (majority direction) and spin-down electrons conduct in parallel with resistivities $\rho_{\uparrow}^{0}$ and $\rho_{\downarrow}^{0}$, respectively. At high temperatures a phonon scattering term ρ_{σ}^{P} is added for each direction of spin, and magnon "spin mixing," characterized by $\rho_{\uparrow\downarrow}$, mingles the two currents. From experimental resistivity data[2,3] ratios $\alpha = \rho_{\downarrow}^{0}/\rho_{\uparrow}^{0}$ characteristic of each impurity have been derived.

Now, for the ordinary Hall effect, we can define a Hall coefficient for each direction of spin R_{σ}^{0}. At low temperatures the well-known two-current formula gives the overall Hall coefficient[8]

$$R_{LT}^{0} = \rho^{2}[R_{\uparrow}^{0}/(\rho_{\uparrow}^{0})^{2} + R_{\downarrow}^{0}/(\rho_{\downarrow}^{0})^{2}], \tag{1}$$

so that for $\alpha \gg 1$, $R_{LT}^{0} \simeq R_{\uparrow}^{0}$.[9] At higher temperatures,

$$R^{0} = \frac{(\rho_{\downarrow} + 2\rho_{\uparrow\downarrow})^{2} R_{\uparrow}^{0} + (\rho_{\uparrow} + 2\rho_{\uparrow\downarrow})^{2} R_{\downarrow}^{0}}{(\rho_{\uparrow} + \rho_{\downarrow} + 4\rho_{\uparrow\downarrow})^{2}}, \tag{2}$$

giving a limiting value (which is also the value for $\alpha = 1$ at low temperature)

$$R_{HT} = (R_{\uparrow}^{0} + R_{\downarrow}^{0})/4. \tag{3}$$

Using these expressions, we can analyze the data of Huguenin and Rivier[10] on dilute Ni:Fe, Fig. 1, knowing $\alpha \simeq 20$ for Fe in Ni.[2] The initial steep fall in R^{0} (4.2°K) as a function of Fe concentration C is a parasitic effect due to the existence of other impurities in the Ni; as Fe is added, the α values for the samples change from $\alpha \simeq 1$, $R^{0} \simeq R_{HT}^{0}$ (residual-impurity dominated) at $C = 0$ to $\alpha \simeq 20$, $R^{0} \simeq R_{\uparrow}^{0}$ (Fe dominated) for $C > 0.5\%$. From values above this concentration it can be seen that R_{LT}^{0}, hence $R_{\uparrow}^{0}$, varies linearly with C, from a value of about zero for $C = 0$. From this value, the high-temperature data, and Eq. (3) we can now estimate $R_{\downarrow}^{0} \simeq -2.4 \times 10^{-10}$ m^{3}/A sec; so the spin-down Fermi surface is dominantly

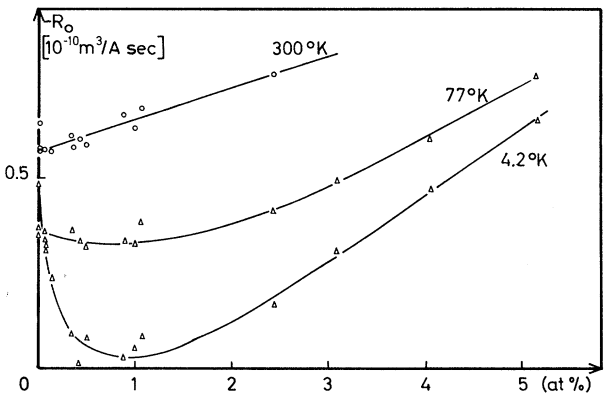

FIG. 1. The ordinary Hall coefficient R_0 as a function of concentration for Ni:Fe alloys (Ref. 9).